

# Quantifying the performance of state of the art sensors to measure guided elastic waves

G.J.A van Groenestijn  
TNO  
The Hague, The Netherlands  
gert-jan.vangroenestijn@tno.nl

T.H. Jansen  
TNO  
Delft, The Netherlands  
rob.jansen@tno.nl

P.L.M.J. van Neer  
TNO / Delft University of Technology  
The Hague / Delft, The Netherlands  
paul.vanneer@tno.nl

M.J. Jacobs  
Optics11  
Amsterdam, The Netherlands  
mark.jacobs@optics11.com

L.K. Cheng  
TNO  
Delft, The Netherlands  
lun.cheng@tno.nl

**Abstract**— Elastic guided waves are carriers of information of the (change in) condition of plate-like structures like wind-turbine blades, airplane wings and road surfaces on bridges. To measure these guided waves we do not have to use piezos. Other sensors offer interesting benefits like contactless sensing, embedding, or measuring without electricity. However, quantitatively comparing them is not trivial: the sensors all have different geometries, operating principles and are sensitive to different mode shapes of guided waves. We designed and performed an experiment to quantitatively compare the performance of five state of the art sensors (piezo, in-fiber interferometer, FBG, free-space interferometer, and ring resonator sensors) to measure  $S_0$  and  $A_0$  guided elastic waves. The measurements were performed on guided waves in an 8 mm steel plate, in the 60-150 kHz range. The dimensions of the plate and the positioning of the sources and sensors was chosen such that the  $S_0$  and  $A_0$  waves arrived in separate time windows. The in-fiber interferometer was the sensor that came closest to the piezo, that was used as reference sensor (-11 dB difference in SNR), the other optical based sensors have SNR values below -30 dB compared to the piezo. The measurements and simulations show that it is important to have two quantitative SNR measures for the performance to measure guided waves: one for the  $S_0$  and one for the  $A_0$  wave. For one sensor we found a difference of 22 dB between these two SNR measures.

**Keywords**— *Ultrasound, Guided waves,  $A_0$  wave,  $S_0$  wave, Piezo, Fiber Bragg Grating, In-fiber Interferometer, Ring Resonator, Free-space Interferometer*

## I. INTRODUCTION

Nowadays there are sensors available that can measure guided waves with interesting extra benefits: fiber Bragg gratings (FBGs) can be embedded, free-space interferometers can measure contactless, and e.g. in-fiber interferometers and ring resonators can measure without electricity. To be able to make the right choices in the design of measurement applications we need quantitative SNR information of sensors. Although, the reception of guided waves has been reported using the above mentioned sensors, it is not trivial to compare the reported performance of these sensors. The performance is different because of the different working principles of the sensors. Also the mode shapes of the different wave modes are complex and differ compared to the fundamental measurement direction of the sensor. Therefore, for a particular application one needs to know which signal a sensor has to measure and one needs a comparison measure.

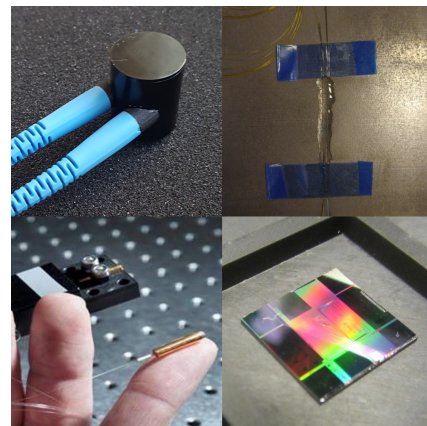


Figure 1. (top left) In-fiber interferometer. (top right) FBG glued on steel plate. (bottom left) Free space interferometers on top of a finger and placed in a black holder. (bottom right) Ring resonator of 13 mm x14 mm.

Our simulations will illustrate that an  $A_0$  wave has significantly more out-of-plane particle displacement than an  $S_0$  wave. Sensors that are more sensitive to out-of-plane particle displacement (like a free-space interferometer measuring perpendicular to the surface) will therefore compare more favorable in terms of SNR in measuring  $A_0$  waves compared to  $S_0$  waves.

In this work we quantitatively compare five sensor types presented in literature: piezo, in-fiber interferometer (Figure 1, top left), FBG (top right), free-space interferometer (bottom left), and ring resonator (bottom, right) sensors in their ability to receive  $S_0$  and  $A_0$  guided waves. This will result in two SNR values (one for the  $S_0$  and one for the  $A_0$  wave) for each of the five sensors.

The comparison measurements will be performed on a steel plate of 8 mm, as this is a common material and thickness to test in the NDT industry. The  $S_0$  and  $A_0$  waves are a logic choice to study as they are used in the majority of guided wave based measurement applications. In our setup they can be isolated from the other signals by their frequency content and velocity.

This paper will begin with some theory on guided waves, followed by the introduction of the five sensors. It will explain the design of the measurement setup and method based on simulations. The paper finalizes with the obtained results and conclusions.

## II. THEORY

### A. Guided waves

In steel plates many types of guided waves can be excited and measured. The particle displacements as function of time caused by these guided waves are differently. Waves that cause particle displacements both in the out-of-plane and in-plane longitudinal direction are called Lamb waves.

Lamb waves that are symmetric with respect to the middle of the plate (i.e. if a particle on top of the plate moves upward, its counterpart at the bottom moves downward) are called S-waves. Waves with antisymmetric particles displacement are called A-waves. With increasing frequency more and more S-wave and A-wave modes will start to appear (Figure 2). The only S-wave and A-wave that exist at low frequencies ( $< 200$  kHz, in an 8mm steel plate) are called the  $S_0$  wave respectively  $A_0$  wave. The velocity of the  $S_0$  and  $A_0$  waves differs and depends on the frequency, the thickness of the plate and the stiffness of the plate.

It is important to isolate and classify the type of guided wave of interest in the measurement data, in order to extract information from it. E.g. in the case of a measured guided wave that was excited by the formation of a crack in a wind-turbine blade, one needs to know the type of guided wave, to know the right velocity needed to locate the crack.

The difference in particle motion between  $S_0$  and  $A_0$  waves can be illustrated by the simulations that were performed in the design phase of the experiment. This was done to determine which frequencies to use and at which distance to place the source and sensor in order to make isolation and classification possible. Figure 3 shows the simulated out-of-plane (blue line) and in-plane (red line) particle displacement for the selected distance and frequency range in our setup. The input wavelet to the source was centered around 90 kHz. The sensor was located 60 cm apart from the source. The first event in the simulated signals appears around 90  $\mu$ s. This is the  $S_0$  wave. Its in-plane particle displacement is larger than its out-of-plane motion, as can be clearly seen. The in-plane and out-of-plane particle motion that make up the  $A_0$  wave, arriving around 170  $\mu$ s, are more equal in magnitude.

### B. Sensors

In this paper we compare the five following sensors:

1) Piezo element (Pz27, Ferroperm Piezoceramics, thickness 2mm, diameter 6.35 mm). A piezo element

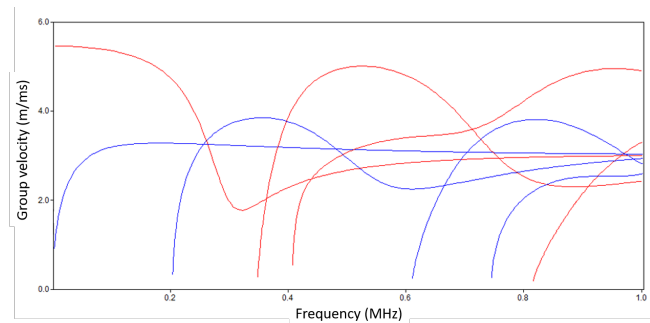


Figure 2. Dispersion curves of symmetric waves (red) and anti-symmetric waves (blue) in an 8 mm steel plate.

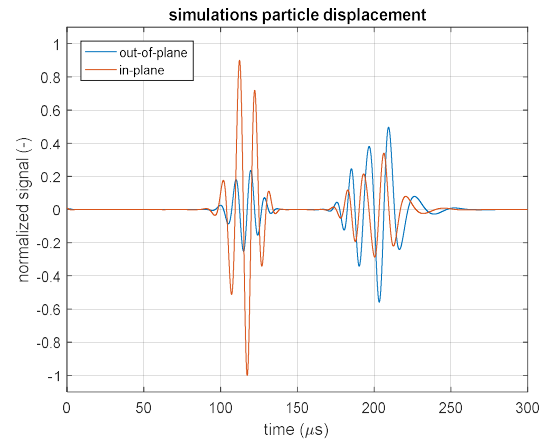


Figure 3. Simulated out-of-plane (blue) and in-plane longitudinal (red) particle displacement on top of an 8 mm steel plate, at a location 60 cm away from the source.

transforms a mechanical stress into an electrical potential and vice versa. A piezo is retrofitted to the measurement object by gluing it to the plate. The piezo element is used as the reference sensor.

2) The in-fiber interferometer [1] (ZS-AEv2, Optics11, see Figure 1) consists of two FBGs. An FBG is a type of distributed Bragg reflector constructed in a short segment of optical fiber that reflects particular wavelengths of light and transmits all others. For the sensor just a reflection of both wavelengths is required, as the phase shift of the returning light is evaluated and not the wavelength shift of the FBG. The principle of the sensor is measuring the change in length of the fiber between two FBGs in the fiber using interferometry. This signal is compared to a stable optical path matching reference fiber. The sensor consists of a sensitive mandrel and a non-sensitive mandrel wrapped with fiber (with FBGs) of the measuring arm and the reference arm respectively. The fiber is only glued on the beginning and ending of the mandrels, leaving the FBGs reflectors unaffected. The sensing mandrel is glued to the target. Local strains or deformation will change the shape of the mandrel and hence introduce a length change in the sensing fiber.

3) The FBG [2] used in this work is a standard type of FBG. The center wavelength will change if a mechanical strain is applied to the FBG. The strain to wavelength coefficient is about  $1.2 \text{ pm}/\mu\epsilon$ . The FBG can be used to measure the strain of the target directly and has inherent the feature of multiple FBG sensor for the realization of a sensor network using a single fiber. For the detection of the FBG wavelength shift a TNO fiber interferometer based high-speed interrogation system is used. The wavelength noise level of this interrogation system is measured to be about  $-150 \text{ dB nm}/\sqrt{\text{Hz}}$ . The current system has a sampling frequency of 1 MHz. An interesting application of FBG sensors is that due to the small fiber diameter of about 0.1 mm, they can be embedded in a medium to measure internal strain. The FBGs were retrofitted to the measurement object.

4) An optical ring resonator [3] (TNO design, manufactured by IMEC) is a set of waveguides in which at least one is a closed loop coupled to a light input and output. The stretching or skewing of the waveguide by guided waves leads to a detectable wavelength shift. Ring resonators were retrofitted to the measurement object.

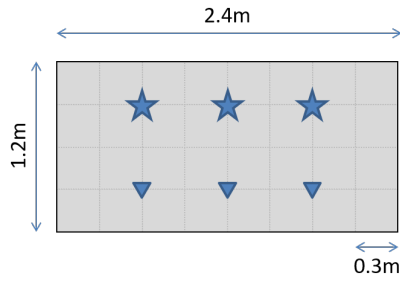


Figure 4. Sketch of the positioning of the sources (stars) and sensors (triangles) on the steel plate

5) A TNO free-space fiber interferometer [4] (also frequently referred to as laser interferometer) emits a laser beam on the measurement surface. A part of the laser light reflects from the measurement surface back into the fiber interferometer. The shift in phase of the interferometer signal is determined and is used as a measure of the displacements on the measurement surface. A fiber interferometer can measure contact free, given the surface diffracts enough light. The diffraction of the surface can be increased by gluing diffracting particles on the surface.

### III. EXPERIMENTAL SETUP AND METHOD

#### A. Set up

Figure 4 shows a sketch of the measurement set-up. As can be seen the plate was large enough to include three source-sensor pairs. The positioning of the source and sensor away from the edges was chosen such that signals that reflect at the edges of the plate were arriving after the signals of interest. On the source-side of the setup equipment (the arbitrary waveform generator (Agilent 33250, Keysight), power amplifier (Krohn-Hite 7500), source piezos (Pz27, Ferroperm Piezoceramics, thickness 2mm, diameter 6.35 mm), and the A/D card (MI.4032, Spectrum) that was also used for triggering) was kept the same for every experiment. On the receiver-side things changed for the five sensors:

1) The signal of the piezo sensor was amplified with an SR560 (Stanford Research) and recorded with the MI.4032 A/D card (Spectrum).

2) The ZonaSens Development kit (Optics11) was used to read out the in-fiber interferometer. The signals of the in-fiber interferometer were received and recorded on a laptop (Optics11).

3) The FBG fiber was positioned parallel to the wave direction. The length of the FBG is  $\sim 8$  mm and the sensing part is directly glued on the metal surface to minimize the influence to the acoustic wave propagating in the sample. The TNO interferometer based interrogator was used to read out the FBG. The signals of the FBG were received and recorded with a DAQ unit (TNO).

4) An Agilent 81960A laser (Keysight) was used to read out the Ring resonator. The signals of the ring resonator were received and recorded with a DAQ unit (TNO).

5) Glass beads in glue were sprayed on the measurement location. The fiber interferometer was aligned at the target location of the test sample to perform the contactless measurement. The signals of the fiber interferometer were received and recorded with a DAQ unit (TNO).

#### B. Method

The simulation results (Figure 3) tell us that we can isolate three time windows of interest: a time window with only noise (before  $90 \mu\text{s}$ ), an  $S_0$  time window (between  $90 \mu\text{s}$  and  $170 \mu\text{s}$ ) and an  $A_0$  time window (after  $170 \mu\text{s}$ ). The  $A_0$  time window will in practice also need an upper limit to exclude waves that reflect at the borders of the medium.

The SNR values for the  $S_0$  wave,  $SNR-S_0$ , reported in this paper are calculated by transforming the recordings in the only-noise and  $S_0$  time window to the frequency domain. The average power ratio of the  $S_0$  time window and the only-noise time window over the 60 kHz – 150 kHz range is taken. From this ratio we subtract the ratio found in the piezo measurement, the result is presented as the  $SNR-S_0$  value. The SNR for the  $A_0$  wave,  $SNR-A_0$ , is determined in the same way using the only-noise and  $A_0$  time-window. We use the  $SNR-S_0$  and  $SNR-A_0$  values to quantify each sensor.

Of course, the  $S_0$  and  $A_0$  time windows also contain noise. To have meaningful SNR values it is required that the noise is at least 20 dB lower than the  $S_0$  or  $A_0$  waves. To fulfill the requirement we use a  $400 \mu\text{s}$  long sweep and measure multiple times, (200, 210, 20000, 2000, 2000 times for respectively piezo, in-fiber interferometer, FBG, free-space interferometer, and ring resonator) ensuring no energy of the previous measurement is recorded in the current one. After averaging of the measurements, the sweep is transformed back (via a correlation) into a pulse in the postprocessing. The  $SNR-S_0$  and  $SNR-A_0$  values are corrected for the number of averaged measurements in case these are different.

### IV. RESULTS

#### A. $SNR-S_0$ and $SNR-A_0$

Figure 5 shows the piezo signal (blue) and the FBG reference fiber signal (red). These signals have been obtained after the processing steps that transformed the sweep into a Gaussian pulse, and averaged over all measurements. The signals of the FBG and piezo are different, because their geometry and sensitivity to in-plane and out-of-plane are different. The  $S_0$  can be isolated in time ( $90 \mu\text{s} - 170 \mu\text{s}$ ). Also, clearly visible is the recorded noise before the  $S_0$  wave arrives in the case of the FBG. The noise recorded before the  $S_0$  wave in the piezo case is at this scale not visible. The  $A_0$  wave ( $170 \mu\text{s} - 210 \mu\text{s}$ ) is harder to isolate than the  $S_0$  wave due to a reflection of an  $S_0$  wave directly arriving behind ( $210 \mu\text{s}$ ) the  $A_0$  wave.

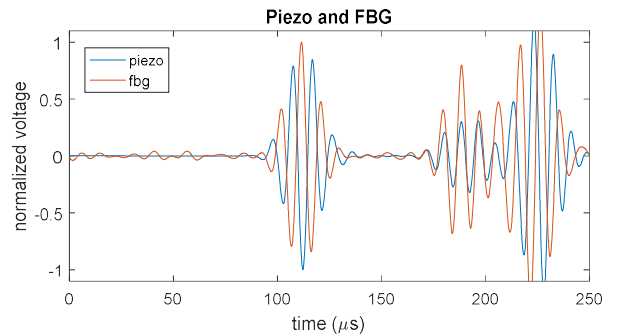


Figure 5. Measured signal of the piezo sensor and FBG with reference grating sensor.

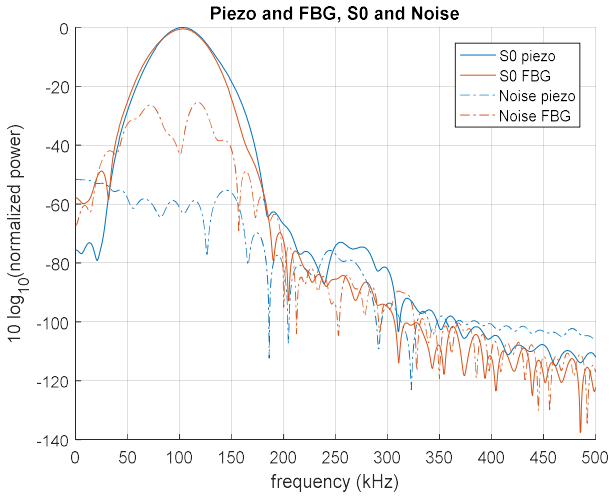


Figure 6. Frequency spectrum of the  $S_0$  wave and noise time window in the piezo and FBG with reference grating measurement

The difference in noise levels between the FBG and piezo is better observed on a log scale in the frequency domain (Figure 6). The noise spectrum is characterized by the correlation of the sweep signal (causing higher amplitudes around 100 kHz) and truncation effects of the time windowing (observed as notches). The difference in the noise level in Figure 6 between the FBG and the piezo 60 kHz – 150 kHz range is 31 dB. However, this was before correcting for the difference in the number of measurements used for averaging. After this correction the  $SNR-S_0$  difference was 51 dB between the FBG and the piezo. Table I summarizes the  $SNR-S_0$  and  $SNR-A_0$  results relative to the piezo for all measured sensors. All optical based sensors measure a better  $SNR-A_0$  than  $SNR-S_0$ . This is partly due to the fact that the piezo is more sensitive to in-plane than out-of-plane displacement, and therefore, in the reference measurement (the piezo) the  $S_0$  wave had a better SNR than the  $A_0$  wave.

From Table I it is clear that the piezo outperforms all other sensors in terms of SNR in measuring both the  $S_0$  and  $A_0$  waves. The in-fiber interferometer is the optical based sensor with the highest  $SNR-S_0$  (-11 dB). It is interesting to note that this is the second generation of this sensor. The first generation only had an  $SNR-S_0$  of -32 dB relative to the piezo. This might indicate the room for improvements for the other optical based sensors.

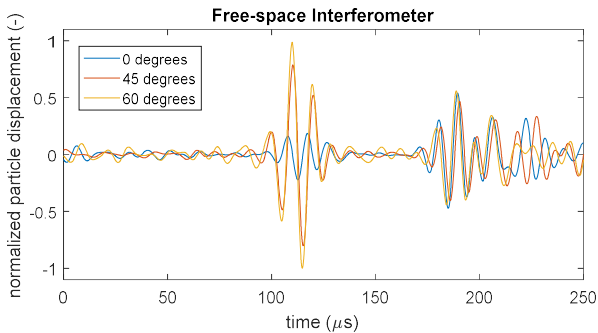


Figure 7. Measured signal of the free-space interferometer positioned under different angles.

TABLE I. SNR values for  $S_0$  and  $A_0$  waves of different sensors.

Sensor	Positioning	$SNR S_0$	$SNR A_0$
Piezo (= reference sensor)	Retrofit	0 dB	0 dB
In-fiber interferom., 2 <sup>nd</sup> gen.	Retrofit	-11 dB	-7 dB
In-fiber interferom., 1 <sup>st</sup> gen.	Retrofit	-32 dB	-16 dB
Free-space interferometer, 45°	Contact less	-42 dB	-35 dB
Free-space interferometer, 60°	Contact less	-46 dB	-40 dB
Ring resonator	Retrofit	-47 dB	-34 dB
FBG	Retrofit/Embed.	-51 dB	-42 dB
Free-space interferometer, 0°	Contact less	-56 dB	-34 dB

### B. Particle displacement

Table I also shows that the  $SNR-S_0$  and  $SNR-A_0$  values can differ significantly, especially for the free-space interferometer. Figure 7 shows three measurements of the free-space interferometer. In each measurement the free-space interferometer measured the receiver location under a different angle. The angle is located in the plain spanned by the normal to the plate (angle = 0 degrees) and the line between the source and the sensor (angle = 90 degrees). It is clearly visible that the measured amplitude of the  $S_0$  wave (90  $\mu$ s - 170  $\mu$ s) depends on the angle. The in-plane particle displacement of an  $S_0$  wave is much stronger than the out-of-plane component. This in contrast to the  $A_0$  wave that depends less on the angle as its out-of-plane and in-plane particle displacements are more or less equal in magnitude (see Figure 3). The  $SNR-S_0$  and  $SNR-A_0$  difference for the free-space interferometer emphasizes that one needs to know the noise performance of a sensor for the desired signal.

Note that the fiber interferometer measurements of Figure 7 more or less confirm the displacement ratios that we have simulated in Figure 3.

## V. CONCLUSION

Using a well-defined setup we quantitatively compared the performance, expressed in  $SNR-S_0$  and  $SNR-A_0$ , of five state of the art sensors. The results are in Table I.

The simulations and fiber interferometer measurements of the particle displacements in the in-plane and out-of-plane directions emphasize that one needs to know the sensor performance in measuring the desired signal. Note the 22 dB difference for the free-space interferometer.

Given that piezos are cheap and outperforming the other sensors in a retrofit setting, it seems that other sensors need to look for niche applications (e.g. contactless sensing, embedded, or measuring in electricity-free environment). However, as the improvements of the second generation in-fiber interferometer over its first generation show, this may change quickly.

## ACKNOWLEDGMENT

The authors like to thank E. Boer, P. Harmsma, P. Toet, B. Speet, E. Doppenberg, L. Schriek, T. Russchenberg, W. Peters, J. Kuijt, A. Sielecki, and C. Arora for their contributions to the measurements.

## REFERENCES

- [1] All-optical fiber sensors for acoustic emission monitoring, Optics11 app note, 2018
- [2] [https://en.wikipedia.org/wiki/Fiber\\_Bragg\\_grating](https://en.wikipedia.org/wiki/Fiber_Bragg_grating)
- [3] [https://en.wikipedia.org/wiki/Optical\\_ring\\_resonators](https://en.wikipedia.org/wiki/Optical_ring_resonators)
- [4] Device for measuring an optical path length difference (US2005275846).